

OPEN

# Uptake of Gadolinium-Based Contrast Agents by Blood Cells During Contrast-Enhanced MRI Examination

Nico Ruprecht, PhD, Dixy Parakkattel, MSci, Lukas Hofmann, PhD, Peter Broekmann, PhD, Nicola Lüdi, DIPL, Christoph Kempf, PhD, Johannes Thomas Heverhagen, MD, PhD, and Hendrik von Tengge-Kobligk, MD

**Objectives:** Gadolinium-based contrast agents (GBCAs) are routinely used in magnetic resonance imaging (MRI) examinations. However, there is limited knowledge about the interaction with and distribution of the drug in human cells. This lack of knowledge is surprising, given that the first interaction of the drug occurs with blood cells. Moreover, recent studies reported gadolinium (Gd) deposition within organs, such as the brain. Hence, this study is aiming to determine the uptake of GBCA in blood cells of patients undergoing contrast-enhanced MRI (ce-MRI) examination.

**Materials and Methods:** Human blood was exposed to either gadoterate meglumine (Gd-DOTA) or Eu-DOTA in vitro or was collected from patients undergoing ce-MRI with Gd-DOTA. Uptake of contrast agents (CAs) by blood cells was quantified by Gd measurements using single-cell inductively coupled plasma mass spectrometry (SC-ICP-MS) or, to confirm Gd-DOTA uptake, by a complementary method using Eu-DOTA by time-resolved fluorescence spectroscopy, respectively.

**Results:** Uptake of Gd-DOTA or Eu-DOTA into white blood cells (WBCs) ex vivo was detectable by SC-ICP-MS and time-resolved fluorescence spectroscopy. The intracellular concentrations were estimated to be in the range of 1–3  $\mu\text{M}$ . However, no CA uptake into erythrocytes was detected with either method. In total, 42 patients between 30 and 84 years old (24 men, 18 women) were enrolled. White blood cells' uptake of Gd was measured by SC-ICP-MS. Isolated WBCs from patients who underwent ce-MRI examination showed substantial Gd uptake; however, the studied patient group showed an inhomogeneous distribution of Gd uptake. Measurements immediately after MRI examination indicated 21–444 attogram/WBC, corresponding to an intracellular Gd concentration in the range from 0.2 to 5.5  $\mu\text{M}$ .

**Conclusions:** This study confirms the ex vivo uptake of GBCA by WBCs and provides the first evidence that GBCA is indeed taken up by WBCs in vivo by patients undergoing ce-MRI examination. However, the observed Gd uptake in WBCs does not follow a log-normal distribution commonly observed in the fields of environmental studies, biology, and medicine. Whether cellular uptake of

GBCA is linked to the observed deposition of Gd remains unclear. Therefore, studying the interaction between GBCA and human cells may clarify crucial questions about the effects of Gd on patients after MRI examinations.

**Key Words:** MRI, SC-ICP-MS, blood cells, contrast agent, patients, gadoteric acid (*Invest Radiol* 2024;00: 00–00)

Gadolinium-based contrast agents (GBCAs) are commonly used for enhanced magnetic resonance imaging (MRI) examinations since the late 1980s.<sup>1</sup> To date, millions of GBCA doses have been administered worldwide and were well tolerated by the majority of patients. However, in 2006, frequent and/or high-dose application of contrast agents (CAs) in some patients with severe renal insufficiency led to a rare systemic disease called nephrogenic systemic fibrosis (NSF).<sup>2</sup> Although the precise pathogenesis of the observed fibrosis remains enigmatic, deposits of gadolinium (Gd) in various tissues and organs have been shown to be responsible for the clinical characteristics of this potentially life-threatening disease.<sup>3,4</sup> In addition to NSF, another severe immune reaction of the immune-mediated inflammatory disease type has manifested itself. It is referred to as Gd deposition disease and considered a type of Gd toxicity.<sup>5,6</sup>

As first described by Kanda et al<sup>7</sup> in 2014, Gd retention in organs can be detected even in patients with intact renal function. The authors observed Gd in cerebral areas (eg, nucleus dentatus and globus pallidus).<sup>7</sup> This finding was also confirmed by several other research groups.<sup>8–14</sup> Moreover, additional evidence emerged over the years that Gd can be found in the brain and other regions of the body, such as neurons or the liver.<sup>15–18</sup> The chemical species of Gd retention remains unknown (ie, as intact chelate, Gd bound to molecules within the organism or as both).<sup>19</sup>

The key question regarding interaction of GBCA on a cellular and molecular level was rarely studied, and current literature remains controversial. If human cells take up GBCA was only sparsely investigated by a few studies to date. Gd<sup>3+</sup> from both Gd-DOTA and Gd-HPDO3A is taken up by rat glioma cells at minuscule levels.<sup>20</sup> Recently, a study concluded that GBCA is present in small amounts in both erythrocytes and leukocytes.<sup>21</sup> Under certain circumstances, these intracellular GBCAs may interfere with cellular metabolism, most probably because of the chemical similarity between Gd and Ca ions. Toxic effects of GBCA were observed in human basal ganglia neurons. There, the CA impairs proper function of mitochondrial respiratory function and cell viability.<sup>15</sup>

As described previously, recent studies revealed Gd deposition in the brain, thereby contradicting the assumption that GBCAs do not cross the functional blood-brain barrier and is immediately excreted from the CNS via venous outflow.<sup>22,23</sup> These fundamental controversies demonstrate that accumulation and deposition of Gd in tissues are—although being of paramount interest—not yet fully understood.

The development and introduction of single-particle inductively coupled plasma mass spectrometry (SP-ICP-MS) opened a new area of research enabling rapid detection and analysis of metal-based particles in a variety of matrices.<sup>24</sup> A continuous development of this method led to applications to cells, termed single-cell ICP-MS (SC-ICP-MS),

Received for publication June 19, 2023; and accepted for publication, after revision, August 15, 2023.

From the Department of Diagnostic, Interventional, and Pediatric Radiology, Bern University Hospital, University of Bern, Bern, Switzerland (N.R., D.P., C.K., J.T.H., H.v.T.-K.); Experimental Radiology Laboratory, Department of BioMedical Research, University of Bern, Bern, Switzerland (N.R., D.P., C.K., J.T.H., H.v.T.-K.); Department of Chemistry, Faculty of Exact Sciences and Institute of Nanotechnology and Advanced Materials, Bar Ilan University, Israel (L.H.); and Department of Chemistry, Biochemistry and Pharmaceutical Sciences (DCBP), University of Bern, Bern, Switzerland (P.B., N.L.).

J.T.H. and H.v.T.-K. share the senior authorship.

Conflicts of interest and sources of funding: The authors declare no conflict of interest.

This research was partially founded by the Swiss National Science Foundation.

This work was supported in part by SNF grant 310030\_215683.

Correspondence to: Nico Ruprecht, PhD, Department of Diagnostic, Interventional, and Pediatric Radiology, Inselspital, Bern University Hospital, Freiburgstrasse 10, 3010 Bern, Switzerland. E-mail: nicoolivier.ruprecht@insel.ch.

Supplemental digital contents are available for this article. Direct URL citations appear in the printed text and are provided in the HTML and PDF versions of this article on the journal's Web site ([www.investigativeradiology.com](http://www.investigativeradiology.com)).

Copyright © 2023 The Author(s). Published by Wolters Kluwer Health, Inc. This is an open-access article distributed under the terms of the Creative Commons Attribution-Non Commercial-No Derivatives License 4.0 (CCBY-NC-ND), where it is permissible to download and share the work provided it is properly cited. The work cannot be changed in any way or used commercially without permission from the journal.

ISSN: 0020-9996/24/0000-0000

DOI: 10.1097/RLI.0000000000001029

thus allowing measurement of intracellular or cell-associated metal ions also within cell organelles, such as the nuclei.<sup>25,26</sup> Based on previous experience in SC-ICP-MS, we investigate the uptake of Gd-DOTA by white blood cells (WBCs).

## MATERIALS AND METHODS

### Materials and Chemicals

Commercialized form of Gd-DOTA (Guerbet, France) was obtained from the Insel Hospital Pharmacy (Bern, Switzerland). Eu-DOTA was purchased from Jena Bioscience (Jena, Germany). Adogen 464, cetyltrimethylammonium chloride, Eu<sup>3+</sup> chloride hexahydrate, Ficoll PM70, Histopaque 1077, Gd<sup>3+</sup> chloride hexahydrate, sodium acetate, sodium chloride, 2-thenoyltrifluoroacetone, and Tween 20 were obtained from Sigma-Aldrich (St Louis, MO). eBioscience 1-Step Fix/Lyse solution was obtained from Invitrogen (Carlsbad, CA). For ex vivo experiments, human blood was purchased from Swiss Transfusion SRC (Bern, Switzerland). For the in vivo experiments, blood samples and written informed consent were obtained from patients who underwent GBCA enhanced MRI examination and participated in a study approved by the cantonal ethics committee of Bern (BASEC ID 2022-00872). All studies were conducted in accordance with the Code of Ethics of the World Medical Association (Declaration of Helsinki) for experiments involving humans.

### Methods

#### Ex Vivo Experiments

Human blood was incubated at 37°C with either 2 mM Gd-DOTA or 2 mM Eu-DOTA (final concentration in blood) under continuous shaking for either 0, 15, 30, or 60 minutes. Subsequently, erythrocytes were isolated either by centrifugation through a Ficoll solution (40 g Ficoll PM70 and 180 mL 0.13 M phosphate buffer) or according to standard protocols using Histopaque 1077.<sup>27</sup> Purified WBCs were obtained with the Histopaque protocol or alternatively by lysis of erythrocytes with eBioscience 1-Step Fix/Lyse solution and subsequent washing of WBCs with phosphate buffered saline (PBS) according to the manufacturer's manual. To determine the kinetics of Gd uptake by WBCs, the measured Gd levels in WBCs at different time points since incubation start were plotted, and the curves were calculated by nonlinear hyperbolic curve fitting using GraphPad Prism software (La Jolla, CA).

To confirm the SC-ICP-MS data, an alternative method of the metal detection was applied, namely, time-resolved fluorescence measurement of the metal ion.<sup>28</sup> For fluorescence measurement of Eu-DOTA, blood from 3 volunteer donors was incubated for 0 or 60 minutes in the presence of 2 mM Eu-DOTA. Erythrocytes and WBCs were isolated and processed as described previously. Fifty microliters of packed erythrocytes was diluted with 50  $\mu$ L H<sub>2</sub>O and 100  $\mu$ L 6 M HCl and incubated for 2 hours at 70°C to dissociate the Eu<sup>3+</sup> from the DOTA macrocycle.<sup>29,30</sup> Subsequently, this solution was transferred to a glass fiber High-Speed Mini Plasmid Column (IBI Scientific, Dubuque, IA) and spun for 30 seconds in a mini-centrifuge (Gilson GmCLab, Middleton, WI) to remove precipitated proteins. The clear solution was then used for Eu<sup>3+</sup> determination by time-resolved fluorescence.

Accordingly, pelleted WBCs were resuspended in 100  $\mu$ L 3 M HCl solution at a concentration of approximately  $2 \times 10^6$  to  $5 \times 10^6$  cells mL<sup>-1</sup> and processed as described previously. Cell densities and diameters were determined using Countess 3 FL Automated Cell Counter (Thermo Scientific, Waltham, MA) according to manufacturer instructions.

Eu<sup>3+</sup> contents were quantified by time-resolved fluorescence measurements essentially as described by Degan et al.<sup>31</sup> Calibration standards were prepared from a 100  $\mu$ M EuCl<sub>3</sub> solution as serial dilutions in H<sub>2</sub>O. Samples (10  $\mu$ L) were mixed with 1 mL enhancement solution composed of 110.5  $\mu$ M 2-thenoyltrifluoroacetone, 1.6 mM Adogen 464, 0.1% Tween 20, 0.5 M NaCl, and 0.1 M Na-acetate, pH 4.45. Time-resolved fluorescence spectroscopy (TRF) spectra be-

tween 550 and 650 nm or emission at 618 nm were recorded on an InfinitePro200 plate reader at an excitation wavelength of 358 nm with a lag time of 400 microseconds and 400 microseconds integration time. The data from i-Control software (Tecan, Männedorf, Switzerland) were transferred to GraphPad Prism to depict the fluorescence spectra and calculate the area under the curve. After building a linear calibration curve with the known concentration values, the cellular Eu<sup>3+</sup> concentration was determined by interpolation.

For SC-ICP-MS measurements, either pelleted erythrocytes or WBCs from whole blood exposed to Gd-DOTA, as described previously, were resuspended in PBS to a concentration of approximately  $4 \times 10^5$  cells mL<sup>-1</sup>. Immediately before measurement on a NexION 2000 ICP-MS instrument (PerkinElmer, Waltham, MA), the resuspended cells were diluted 1:4 in H<sub>2</sub>O, as described previously.<sup>26</sup> Single-cell ICP-MS experiments were performed using PerkinElmer's NexION 2000 ICP-MS, which was set up with specific material for single-cell experiments as described previously.<sup>26</sup> The transport efficiency was calibrated with 50-nm gold nanoparticles (NanoComposix, San Diego, CA) with a concentration of 10<sup>5</sup> particles/mL. The SC-ICP-MS instrument used for total Gd determination was optimized daily with a multi-element standard. The acquired raw data were processed with Syngistix single-cell application software module (PerkinElmer, Waltham, MA).

A positive control for SC-ICP-MS was generated by artificially loading erythrocytes with Gd-DOTA.<sup>32</sup> Briefly, erythrocytes were washed 3 times with PBS; subsequently, 2.5 mL packed erythrocytes were diluted with an equal volume of 10 mM Gd-DOTA in H<sub>2</sub>O and incubated for 30 minutes on ice. Subsequently, 150  $\mu$ L 2.5 M NaCl was added to restore isotonic conditions. The resealed cells were incubated at room temperature for 15 minutes and centrifuged for 20 minutes in a benchtop microcentrifuge. Subsequently, 3.5 mL supernatant was removed and replaced with 4 mL PBS, and resuspended and centrifuged for a further 15 minutes. The supernatant was removed, and the pellet was washed 3 more times with 4 mL PBS. The pelleted erythrocytes (0.5 mL) were mixed with 0.5 mL PBS (denoted as Gd-loaded erythrocytes).

The same procedure was applied for the "negative" control in the absence of Gd-DOTA, thus resulting in mock loaded erythrocytes. To these cells, Gd-DOTA was added with a final concentration of 5 mM, incubated for 30 minutes, centrifuged for 20 minutes, and subsequently washed 4 times with PBS (mock loaded/Gd erythrocytes).

### In Vivo Experiments

Patients undergoing MRI examination with Gd-DOTA were included in the pilot study. Minors, adults incapable of judgment or consent, pregnant or lactating women, or vulnerable people were excluded from the study. Height, weight, and sex were used to estimate the blood volume of each patient according to the Nadler formula.<sup>33</sup> Finally, based on the amount of Gd-DOTA administered, the GBCA concentration in the bloodstream was calculated.

For this study, 5 mL of blood was drawn after MRI examination. Isolation of WBCs and determination of Gd uptake with SC-ICP-MS were performed as described previously. Briefly, immediately after MRI examination, 0.2 mL blood was diluted with Fix/Lysis buffer (Invitrogen) and incubated for 30 minutes; WBCs were subsequently purified by repetitive centrifugation and washing (sample t<sub>x</sub>). Exactly 60 minutes after the patient had received GBCA, a second sample of 0.2 mL of the previously drawn blood was treated with Fix/Lyse solution (sample t<sub>60</sub>). The sample was processed as described previously, too. Subsequently, WBC counts, as well as cell diameter, were measured (Countess 3 FL), and the Gd content per cell was determined with SC-ICP-MS (PerkinElmer). The collected data were stored in a Redcap electronic case report form (including sex, age, weight, height, blood group, date/time of administration of the CA, date/time of blood collection, amount of CA administered, CA name, average amount of Gd per cell, and average cell diameter; see supporting information).

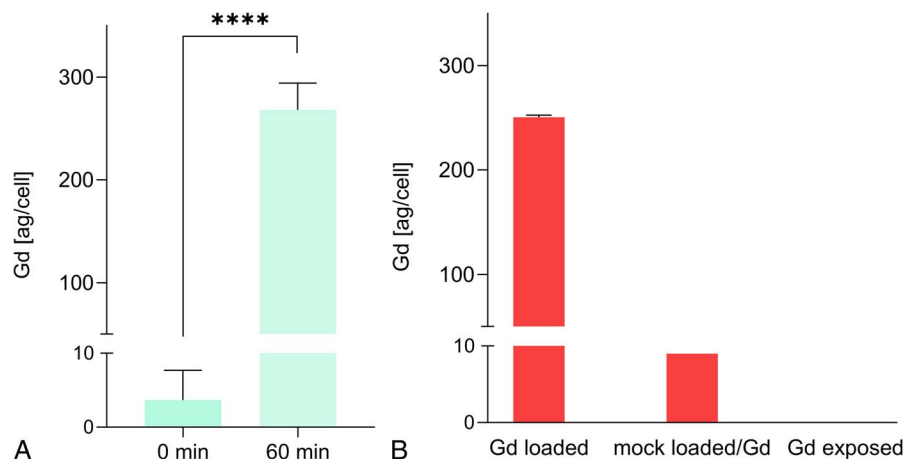


**FIGURE 1.** Determination of the Gd-DOTA uptake in blood cells ex vivo. A, Cellular amount of Gd in WBCs after 60 minutes incubation with 2 mM Gd-DOTA (\*\*\*\* $P < 0.0001$ ). B, Erythrocytes artificially loaded with 5 mM Gd-DOTA using hypotonic buffer (Gd loaded), mock loaded erythrocytes, or incubated with 2 mM Gd-DOTA (Gd exposed). Only erythrocytes artificially loaded with 5 mM Gd-DOTA showed clear uptake by SC-ICP-MS.

### Statistics and Distribution Analysis

Statistical analyses were performed with unpaired 2-tailed  $t$  test. The fit of the distribution of Gd uptake in WBCs to a log-normal distribution was tested with 4 different log-normality tests.<sup>34</sup> In addition, frequency distribution analyses were performed, and nonlinear regression analysis was applied on the results obtained. All operations were performed in GraphPad Prism 8.0 software.

## RESULTS

### Quantification of Gd-DOTA Uptake in Blood Cell Ex Vivo Using SC-ICP-MS

When GBCA is administered to human patients at a concentration of  $0.1 \text{ mmol kg}^{-1}$  bodyweight, the expected CA concentration in the blood may reach approximately 2 mM. Therefore, a final concentration of 2 mM Gd-DOTA or Eu-DOTA was used for the ex vivo experiments.

In a first step, human blood was incubated with Gd-DOTA for 1 hour. Subsequently, the amount of Gd in WBCs and erythrocytes

was determined by SC-ICP-MS. In WBCs of 2 voluntary donors, an average of  $268 \pm 24$  attogram ( $\text{ag} = 10^{-18} \text{ g}$ ) of Gd per cell was measured. The cellular concentration was calculated according to the volume of WBCs, which, for these 2 volunteers, was 570 femtoliter ( $\text{fL} = 10^{-15} \text{ liter}$ ). Application of this volume resulted in an intracellular concentration of approximately  $3 \pm 0.3 \text{ }\mu\text{M}$  (Fig. 1A). No uptake was detected in erythrocytes. Only erythrocytes artificially loaded with 5 mM Gd-DOTA showed a prominent signal in SC-ICP-MS measurements. The low amount of 7 ag in the mock loaded sample originated from incomplete (<100%) resealing of erythrocytes (Fig. 1B).

### Determination of Eu-DOTA Uptake in WBCs or Erythrocytes Ex Vivo Assessed by TRF

To confirm Gd-DOTA uptake, quantification of GBCA uptake was performed by a complementary method using TRF. For this purpose, Gd was replaced with europium (Eu) in the CA (Eu-DOTA). The Eu-DOTA uptake by human WBC cells or erythrocytes after incubation was calculated from the difference in  $\text{Eu}^{3+}$  concentration between the measurements after 0 and 60 minutes incubation time. Values from 3

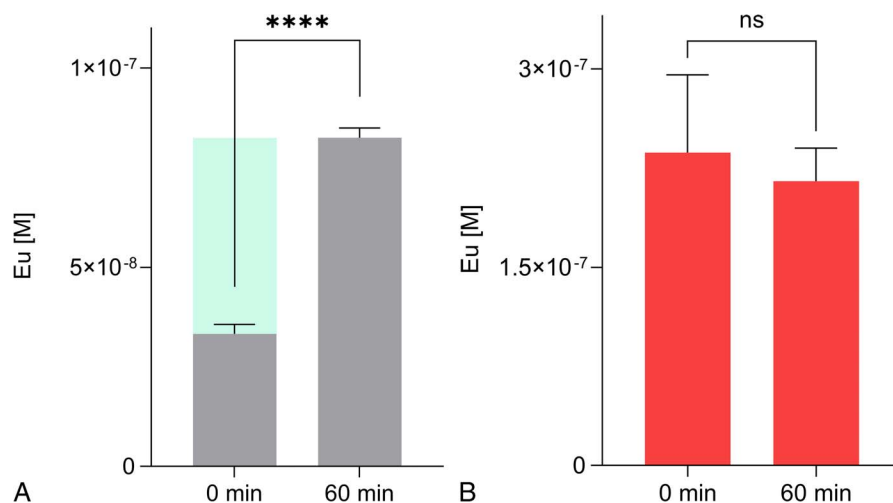


**FIGURE 2.** Eu-DOTA uptake was measured by TRF in erythrocytes and WBCs ex vivo. The graphs show the data of a representative experiment from the blood of a single donor. A, An increase in Eu-DOTA uptake was detected in WBCs. The light green-shaded part represents the amount of Eu uptake by the WBCs and is used to calculate the intracellular concentration (\*\*\*\* $P < 0.0001$ ). B, No increase in Eu-DOTA was detected in erythrocytes (ns indicates not significant).

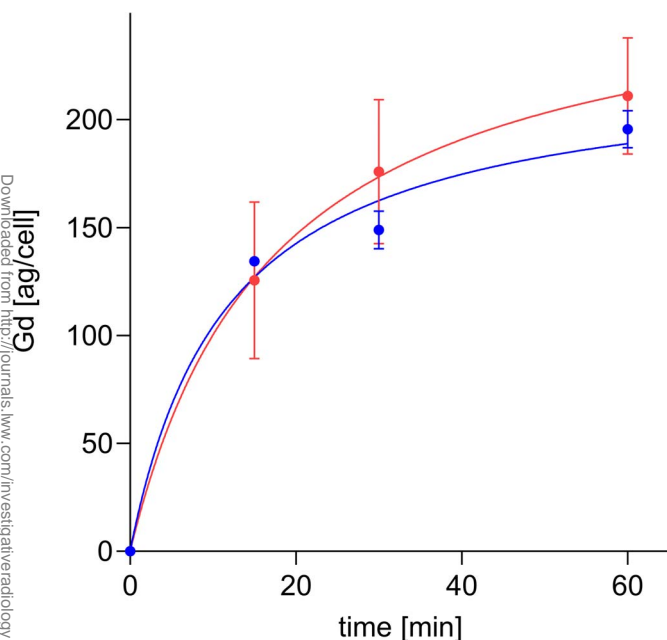


**FIGURE 3.** Timeline of Gd-DOTA uptake in WBCs from 2 different donors. Whole blood of each donor was incubated ex vivo for 0, 15, 30, and 60 minutes with Gd-DOTA at a final concentration of 2 mM. WBCs were isolated, and Gd content was measured by SC-ICP-MS as described in *Materials and Methods*.

independent experiments, representing 3 different donors and containing at least triplicate values, were used. To confirm a significant difference between the means of each single experiment, an unpaired 2-tailed *t* test was performed, resulting in a *P* value < 0.0001. The intracellular  $\text{Eu}^{3+}$  concentration could be calculated based on these differences, by considering the sample volumes, the average cell number used in the experiments, and the mean cell diameter of the WBCs. The WBC diameter was determined to be 10  $\mu\text{m}$  on average, ranging between 9.8 and 10.1  $\mu\text{m}$ . With these parameters, the intracellular  $\text{Eu}^{3+}$  concentrations were estimated to be in the range of 1–3  $\mu\text{M}$  (Fig. 2A). For the details of calculation of the representative example given in this figure, see Figure S1, <http://links.lww.com/RLI/A865>. In the case of erythrocytes, no distinction between the 0 and 60 minutes time points was observed; hence, no uptake was detectable (Fig. 2B).

### Kinetics of Gd-DOTA Uptake in WBCs Ex Vivo, Determined by SC-ICP-MS

Examination of ex vivo Gd-DOTA uptake in WBCs was assessed from 2 donors over 1 hour. The ag/cell values were quantified for 2 donors. For 1 donor, values of  $126 \pm 36$ ,  $176 \pm 33$ , and  $211 \pm 27$  ag/cell were measured at 15, 30, and 60 minutes, respectively. For the other donor, values of  $134 \pm 2$ ,  $149 \pm 9$ , and  $196 \pm 9$  ag/cell were determined at 15, 30, and 60 minutes, respectively (Fig. 3).

### Uptake of Gd-DOTA in Patients Undergoing ce-MRI

The promising results from ex vivo studies led to the initiation of a clinical pilot study on the uptake of GBCA in patients undergoing contrast-enhanced MRI (ce-MRI) with Gd-DOTA. A total of 42 patients between 30 and 84 years of age (24 men, 18 women) were enrolled in this study. Details such as sex, age, height, weight, and amount of GBCA administered were collected. Based on part of these data, the blood GBCA level was estimated for each patient and resulted in a concentration of 1.5 mM in average (range, 1.2–1.9 mM). For details, see Figures S2–S8, <http://links.lww.com/RLI/A865>, of supporting information. The mean time

from GBCA injection to first fixation  $t_x$  was  $17 \pm 3$  minutes (range, 10–25 minutes) among the 42 patients (Fig. S8, <http://links.lww.com/RLI/A865>, of supporting information). Calculation of Gd uptake in WBCs was determined in all patients by SC-ICP-MS. In 2 patients, uptake of Gd could not be determined at time  $t_x$ , because the values were below the detection limit of 7 ag/cell. In the remaining 40 patients, values between 21 and 444 ag per WBC were measured. At  $t_{60}$ , 25–763 ag per WBC was measured in all 42 patients (Fig. 4). For all patients, an increase in Gd content per cell was also observed between  $t_x$  and  $t_{60}$  (see Fig. S9, <http://links.lww.com/RLI/A865>). Based on WBC diameter and the Gd content/cell, the intracellular Gd concentration was calculated for each patient and time point ( $t_x$  and  $t_{60}$ ). The intracellular Gd concentration was 0.2–5.5  $\mu\text{M}$  for samples at  $t_x$  and 0.4–9.7  $\mu\text{M}$  for samples at  $t_{60}$ , respectively. Hence, the concentrations of intracellular Gd from patients' samples were within the high nanomolar to low micromolar range. These data were further examined to assess a possible correlation between intracellular Gd levels and the GBCA concentration in the blood; the exposure time; and the body mass index, which reflects the patient's height and weight (Figs. S10–S12, <http://links.lww.com/RLI/A865>, of supporting information). However, no correlations were found.

### Distribution Analysis of Gd-DOTA in Patients Undergoing ce-MRI

Gadolinium uptake in WBCs determined by SC-ICP-MS in 42 patient samples showed an inhomogeneous distribution. According to the violin plot (Fig. 4), a log-normal distribution was not apparent.

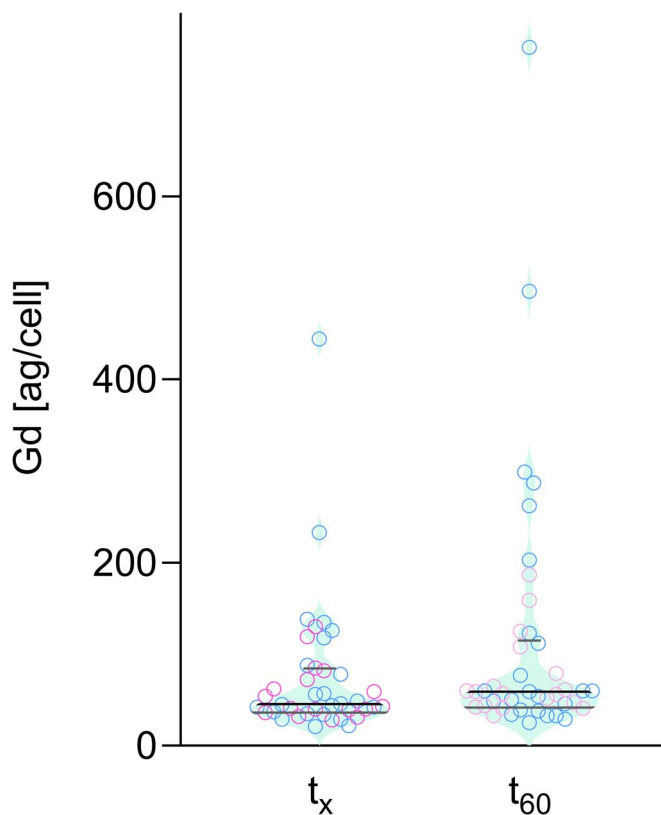


**FIGURE 4.** The uptake of Gd in WBCs was determined in a total of 42 patients who underwent ce-MRI by SC-ICP-MS. In 40 patients, values between 21 and 444 ag per WBC (first quartile = 36 ag, median = 47 ag, third quartile = 84 ag) were measured at time  $t_x$ . At time  $t_{60}$ , 25 to 763 ag (first quartile = 42 ag, median = 59 ag, third quartile = 115 ag) were measured (pink circle = ♀; blue circle = ♂) in 42 patients.

Downloaded from http://journals.lww.com/investigativeradiology by BMDI56P8Kav1Z4Eoutm1K0N44+hk1hEzgo sIH04XMI0h0CymcX1AWNvQpIIQHD3I3DOODRfY7TVSF14C3VC1Y0abpgQZQZG12MwZLel= on 10/13/2023

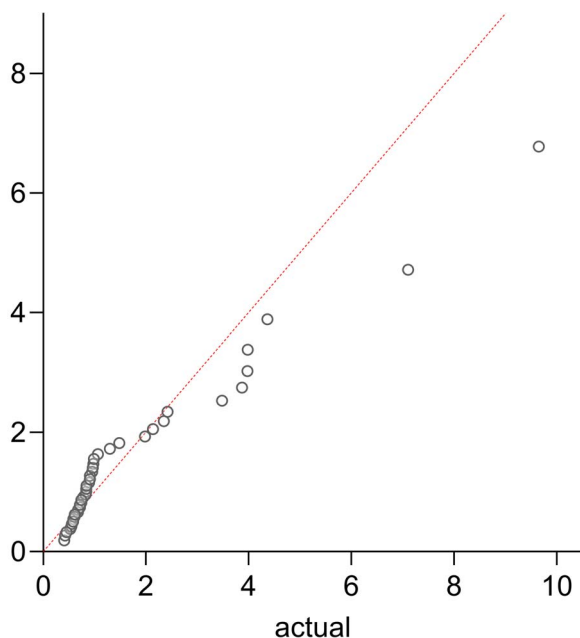


**FIGURE 5.** The quantile-quantile plot shows the comparison of the theoretically predicted values assuming a lognormal distribution (theoretical model) and the effective patient data. Visual comparison of the plotted points (circle) to the reference line (red) plausibly suggests a nonlognormal distribution.

D'Agostino-Pearson, Anderson-Darling, Shapiro-Wilk, and Kolmogorov-Smirnov tests further confirmed this finding: none of the tests supported a log-normal distribution, as indicated in a quantile-quantile plot (Fig. 5). The plot of natural logarithm of cellular Gd concentration in patients' WBCs against the cumulative frequency for the given data exhibited a bimodal character (Fig. 6A). Hence, frequency versus natural logarithm of cellular Gd concentration in patients' WBCs also suggested a bimodal (2 patient populations) rather than a log-normal distribution (Fig. 6B).

### DISCUSSION

Our study indicates that GBCAs are taken up ex vivo by WBCs and demonstrates for the first time in vivo the uptake of GBCAs in WBCs isolated from patients investigated by ce-MRI. An intracellular

concentration of approximately 3  $\mu\text{M}$  was detected ex vivo in WBCs after 1 hour by SC-ICP-MS. These results were confirmed with an orthogonal method, using Eu-DOTA and TRF measurements, which revealed intracellular Eu concentrations in the same low micromolar range as those determined with SC-ICP-MS. Ex vivo uptake studies in WBCs after incubation with 2 mM Gd-DOTA followed a saturation curve. More importantly, in erythrocytes, Gd was not detected by SC-ICP-MS after intact erythrocytes were incubated with GBCA. The detection limit of SC-ICP-MS was approximately 7 ag per cell, corresponding to an approximately 0.5  $\mu\text{M}$  intracellular concentration in erythrocytes. However, when erythrocytes were permeabilized, then incubated with GBCA, subsequently resealed, and finally washed, Gd was clearly detectable. This is convincing evidence that the Gd detected by SC-ICP-MS is within the cellular compartment.

In addition, the concentrations of intracellular Gd in WBCs of patients undergoing ce-MRI were analyzed. Gadolinium uptake in WBCs was determined by SC-ICP-MS immediately after completion of MRI and additionally exactly 1 hour after GBCA administration. Surprisingly, a substantial amount of Gd was already detected in the  $t_x$  samples. Only 2 patients showed no uptake of GBCA in WBCs immediately after MRI. However, Gd was detectable at  $t_{60}$  in all patient samples. The measured intracellular concentration varied among patients from 0.2 to 9.7  $\mu\text{M}$ . Furthermore, the time from GBCA administration to first fixation of the blood sample averaged 17 minutes, showing rapid uptake, as confirmed by the kinetics of the ex vivo studies.

The violin plot of Gd uptake showed a nonhomogeneous distribution. This distribution would be expected to follow a log-normal distribution, as widely observed in the fields of environmental studies, biology, and medicine.<sup>35</sup> However, data analysis with D'Agostino-Pearson, Anderson-Darling, Shapiro-Wilk, and Kolmogorov-Smirnov tests argued against a log-normal distribution. Therefore, we propose that 2 populations exist: one in which WBCs take up Gd at higher concentration than the other. The putative appearance of these 2 groups was already visible at  $t_x$  but became more prominent at  $t_{60}$ . The existence of the 2 groups was evident in the frequency distribution analysis. However, this hypothesis remains to be further investigated and confirmed.

The question of whether GBCAs are taken up by cells has scarcely been investigated. In a recent study, significantly more Gd was detected in WBCs after ex vivo incubation.<sup>21</sup> Concentrations 10–40 times higher than observed in our experiments were reported. Moreover, a prior study showed a linear uptake of the CA over 3 hours. However, our study revealed that the intracellular Gd concentration approached saturation after 1 hour.

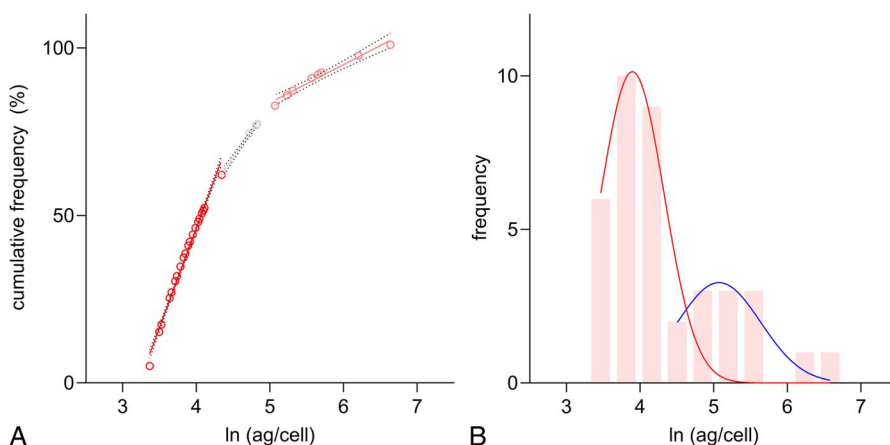


**FIGURE 6.** A, The natural logarithm of the cellular Gd concentration in the patient's WBCs determined after ce-MRI was plotted against the cumulative frequency. For a log-normal distribution, this should result in a straight line. Red: quintiles 1–4, pink: quintile 5. B, Frequency versus the natural logarithm of cellular Gd concentration patient's WBC. A log-normal distribution would result in a single red/blue line: curve fit for quintile 1–3 and quintile 4 assuming a log-normal distribution.

Notably, in the study by Di Gregorio et al,<sup>21</sup> incubation was performed at 5 mM GBCA rather than the 2 mM, which seems to be closer to physiological range and used in the present study. The 2 mM concentration is slightly higher than the average blood concentration calculated from the administered amount of GBCA and the estimated blood volume, calculated with the Nadler formula.<sup>33</sup> In another study, the uptake of GBCA in WBCs was measured by high-resolution magic-angle spinning NMR spectroscopy at an incubation with 1–7.5 mM GBCA. Gadolinium-based contrast agent was detectable only in the extracellular space; hence, the authors claimed that these complexes cannot cross cell membranes.<sup>36</sup> In summary, Gd was detected in WBCs in our study as well as in the study by Di Gregorio et al<sup>21</sup> in contrast to the study by Calabi et al.<sup>36</sup> However, consistent with Calabi et al,<sup>36</sup> no Gd was detected in the erythrocytes.

Thus, our results only partially recapitulate the previously published. At present, we have no provable explanation for this discrepancy and any attempt to do so would be purely speculative. However, it could be speculated, although unlikely, that the net charge of CAs may have an influence on the cellular uptake.

The importance of GBCAs uptake in WBCs should not be underestimated. Intracellular Gd in WBCs has the potential to be distributed throughout the human body. Circulating neutrophils have a short life span of approximately 24 hours and die by constitutive apoptosis and are eliminated by macrophages in the liver, spleen, and bone marrow, where high Gd concentrations are also found.<sup>37–40</sup> Furthermore, during the inflammatory response, WBCs cross the endothelial cell layer at the site of inflammation, allowing the WBCs to eventually enter the tissue.<sup>41,42</sup> Hence, our findings show that the pharmacology of GBCAs is fundamental to our understanding of the basic ADME (absorption, distribution, metabolism, and excretion) properties and the implications of these CAs in patients.

The limitations of the present study are the restricted number of patients and reliance on ex vivo data. The ex vivo data, which were similar for both donors, may just be coincidence and therefore does not allow for any conclusions at this point. Furthermore, the range of intracellular Gd concentrations may increase if larger numbers of patients are analyzed. The patient number studied to date is too small to allow any conclusions to be drawn or to propose any forward-looking hypotheses based on statistical analysis of the data. In addition, the uptake was determined with TRF or SC-ICP-MS. Both methods only detect the metal itself and do not distinguish whether the complex is still intact or whether the Gd or Eu is eventually present in a free or altered form. Clarifying this should be addressed by future studies and is important, especially in view of possible toxic effects of Gd. However, so far, macrocyclic GBCAs were described to be stable under these conditions.<sup>21,43</sup>

In conclusion, this pilot study clearly demonstrates that isolated WBCs from patients undergoing ce-MRI examination showed substantial uptake of Gd. The 42 patients exhibited an inhomogeneous distribution of Gd uptake. Furthermore, descriptive analysis suggested a bimodal (2 patient populations) rather than a log-normal distribution. Any attempt to explain this pattern of intracellular Gd in patient WBCs would be premature and requires further investigation.

Therefore, another prospective study with substantially more patients should be performed to confirm the bimodal or log-normal distribution. Furthermore, an additional study could identify patient-specific cohorts that influence contrast media uptake and ultimately contribute to the understanding of Gd deposition in organs. Finally, these results have implications in the understanding of the biological distribution of CAs, and on the cellular mechanism of action. Ultimately, quantification of cellular uptake of CA might be useful for predicting the safety of newly developed GBCAs.<sup>44,45</sup>

#### ACKNOWLEDGMENTS

The authors thank all participants for their contribution to the study and thank the medical-technical assistants from the radiology department for providing excellent technical support.

#### REFERENCES

- Lohrke J, Frenzel T, Endrikat J, et al. 25 years of contrast-enhanced MRI: developments, current challenges and future perspectives. *Adv Ther.* 2016;33:1–28.
- Khurana A, Runge VM, Narayanan M, et al. Nephrogenic systemic fibrosis: a review of 6 cases temporally related to gadodiamide injection (Omniscan). *Invest Radiol.* 2007;42:139–145.
- Malikova H. Nephrogenic systemic fibrosis: the end of the story? *Quant Imaging Med Surg.* 2019;9:1470–1474.
- Wiginton CD, Kelly B, Oto A, et al. Gadolinium-based contrast exposure, nephrogenic systemic fibrosis, and gadolinium detection in tissue. *AJR Am J Roentgenol.* 2008;190:1060–1068.
- Semelka RC, Ramalho M. Gadolinium deposition disease: current state of knowledge and expert opinion. *Invest Radiol.* 2023;58:523–529.
- Semelka RC, Ramalho M. Commentary on the association of symptoms associated with gadolinium exposure/gadolinium deposition disease and gadolinium-based contrast agents. *Invest Radiol.* 2022;57:674–676.
- Kanda T, Ishii K, Kawaguchi H, et al. High signal intensity in the dentate nucleus and globus pallidus on unenhanced T1-weighted MR images: relationship with increasing cumulative dose of a gadolinium-based contrast material. *Radiology.* 2014;270:834–841.
- Robert P, Violas X, Grand S, et al. Linear gadolinium-based contrast agents are associated with brain gadolinium retention in healthy rats. *Invest Radiol.* 2016;51:73–82.
- Robert P, Fingerhut S, Factor C, et al. One-year retention of gadolinium in the brain: comparison of gadodiamide and gadoterate meglumine in a rodent model. *Radiology.* 2018;288:424–433.
- Gulani V, Calamante F, Shellock FG, et al. Gadolinium deposition in the brain: summary of evidence and recommendations. *Lancet Neurol.* 2017;16:564–570.
- Malhotra A, LeSar B, Wu X, et al. Progressive T1 shortening of the dentate nucleus in patients with multiple sclerosis: result of multiple administrations of linear gadolinium contrast agents versus intrinsic disease. *AJR Am J Roentgenol.* 2018;211:1099–1105.
- Strzeminska I, Factor C, Jimenez-Lamana J, et al. Comprehensive speciation analysis of residual gadolinium in deep cerebellar nuclei in rats repeatedly administered with gadoterate meglumine or gadodiamide. *Invest Radiol.* 2022;57:283–292.
- Quattrocchi CC, Parillo M, Spani F, et al. Skin thickening of the scalp and high signal intensity of dentate nucleus in multiple sclerosis: association with linear versus macrocyclic gadolinium-based contrast agents administration. *Invest Radiol.* 2023;58:223–230.
- Anderhalten L, Silva RV, Morr A, et al. Different impact of gadopentetate and gadobutrol on inflammation-promoted retention and toxicity of gadolinium within the mouse brain. *Invest Radiol.* 2022;57:677–688.
- Bower DV, Richter JK, von Tengge-Kobligk H, et al. Gadolinium-based MRI contrast agents induce mitochondrial toxicity and cell death in human neurons, and toxicity increases with reduced kinetic stability of the agent. *Invest Radiol.* 2019;54:453–463.
- Maximova N, Gregori M, Zennaro F, et al. Hepatic gadolinium deposition and reversibility after contrast agent-enhanced MR imaging of pediatric hematopoietic stem cell transplant recipients. *Radiology.* 2016;281:418–426.
- Gibby WA, Gibby KA, Gibby WA. Comparison of Gd DTPA-BMA (Omniscan) versus Gd HP-DO3A (ProHance) retention in human bone tissue by inductively coupled plasma atomic emission spectroscopy. *Invest Radiol.* 2004;39:138–142.
- Aime S, Caravan P. Biodistribution of gadolinium-based contrast agents, including gadolinium deposition. *J Magn Reson Imaging.* 2009;30:1259–1267.
- Di Gregorio E, Ferrauto G, Furlan C, et al. The issue of gadolinium retained in tissues: insights on the role of metal complex stability by comparing metal uptake in murine tissues upon the concomitant administration of lanthanum- and gadolinium-diethylenetriaminopentaacetate. *Invest Radiol.* 2018;53:167–172.
- Cabella C, Crich SG, Corpillo D, et al. Cellular labeling with Gd(III) chelates: only high thermodynamic stabilities prevent the cells acting as 'sponges' of Gd3+ ions. *Contrast Media Mol Imaging.* 2006;1:23–29.
- Di Gregorio E, Furlan C, Atlante S, et al. Gadolinium retention in erythrocytes and leukocytes from human and murine blood upon treatment with gadolinium-based contrast agents for magnetic resonance imaging. *Invest Radiol.* 2020;55:30–37.
- Rasschaert M, Weller RO, Schroeder JA, et al. Retention of gadolinium in brain parenchyma: pathways for speciation, access, and distribution. A critical review. *J Magn Reson Imaging.* 2020;52:1293–1305.
- McDonald RJ, McDonald JS, Dai D, et al. Comparison of gadolinium concentrations within multiple rat organs after intravenous administration of linear versus macrocyclic gadolinium chelates. *Radiology.* 2017;285:536–545.
- Montano MD, Olesik JW, Barber AG, et al. Single particle ICP-MS: advances toward routine analysis of nanomaterials. *Anal Bioanal Chem.* 2016;408:5053–5074.

25. Corte Rodriguez M, Alvarez-Fernandez Garcia R, Blanco E, et al. Quantitative evaluation of cisplatin uptake in sensitive and resistant individual cells by single-cell ICP-MS (SC-ICP-MS). *Anal Chem*. 2017;89:11491–11497.
26. Gale A, Hofmann L, Ludi N, et al. Beyond single-cell analysis of metalldrugs by ICP-MS: targeting cellular substructures. *Int J Mol Sci*. 2021;22:9468.
27. Merck. Recommended standard method for isolating mononuclear cells. Available at: <https://www.sigmaaldrich.com/CH/de/technical-documents/protocol/clinical-testing-and-diagnostics-manufacturing/hematology/recommended-standard-method>. Accessed November 28, 2022.
28. Gudgin Dickson EF, Pollak A, Diamandis EP. Time-resolved detection of lanthanide luminescence for ultrasensitive bioanalytical assays. *J Photochem Photobiol B Biol*. 1995;27:3–19.
29. De Silva CR, Vagner J, Lynch R, et al. Optimization of time-resolved fluorescence assay for detection of europium-tetraazacyclododecyltetraacetic acid-labeled ligand-receptor interactions. *Anal Biochem*. 2010;398:15–23.
30. Toth E, Brucher E, Lazar I, et al. Kinetics of formation and dissociation of lanthanide(III)-DOTA complexes. *Inorg Chem*. 1994;33:4070–4076.
31. Degan P, Abbondandolo A, Montagnoli G. A new fluorescence enhancement solution for europium-based time-resolved fluorimmunoassays. *J Biolumin Chemilumin*. 1990;5:207–212.
32. Bourgeaux V, Lanao JM, Bax BE, et al. Drug-loaded erythrocytes: on the road toward marketing approval. *Drug Des Devel Ther*. 2016;10:665–676.
33. Nadler SB, Hidalgo JH, Bloch T. Prediction of blood volume in normal human adults. *Surgery*. 1962;51:224–232.
34. D'Agostino RB, Stephens MA. *Goodness-of-Fit Techniques*. New York, NY: Marcel Dekker; 1986.
35. Limpert E, Stahel WA, Abbt M. Log-normal distributions across the sciences: keys and clues: on the charms of statistics, and how mechanical models resembling gambling machines offer a link to a handy way to characterize log-normal distributions, which can provide deeper insight into variability and probability—normal or log-normal: that is the question. *Bioscience*. 2001;51:341–352.
36. Calabi L, Alfieri G, Biondi L, et al. Application of high-resolution magic-angle spinning NMR spectroscopy to define the cell uptake of MRI contrast agents. *J Magn Reson*. 2002;156:222–229.
37. Di Gregorio E, Iani R, Ferrauto G, et al. Gd accumulation in tissues of healthy mice upon repeated administrations of gadodiamide and gadoteridol. *J Trace Elem Med Biol*. 2018;48:239–245.
38. McCracken JM, Allen LA. Regulation of human neutrophil apoptosis and lifespan in health and disease. *J Cell Death*. 2014;7:15–23.
39. Turyanskaya A, Rauwolf M, Pichler V, et al. Detection and imaging of gadolinium accumulation in human bone tissue by micro- and submicro-XRF. *Sci Rep*. 2020;10:6301.
40. Summers C, Rankin SM, Condliffe AM, et al. Neutrophil kinetics in health and disease. *Trends Immunol*. 2010;31:318–324.
41. Muller WA. Getting leukocytes to the site of inflammation. *Vet Pathol*. 2013;50:7–22.
42. Ince LM, Weber J, Scheiermann C. Control of leukocyte trafficking by stress-associated hormones. *Front Immunol*. 2018;9:3143.
43. Frenzel T, Lengsfeld P, Schirmer H, et al. Stability of gadolinium-based magnetic resonance imaging contrast agents in human serum at 37 degrees C. *Invest Radiol*. 2008;43:817–828.
44. Loevner LA, Kolumban B, Hutoczki G, et al. Efficacy and safety of gadopipiclenol for contrast-enhanced MRI of the central nervous system: the PICTURE randomized clinical trial. *Invest Radiol*. 2023;58:307–313.
45. Lohrke J, Berger M, Frenzel T, et al. Preclinical profile of gadoquatrane: a novel tetrameric, macrocyclic high relaxivity gadolinium-based contrast agent. *Invest Radiol*. 2022;57:629–638.